Aerospace Science and Technology 24 (2013) 177–186

Contents lists available at SciVerse ScienceDirect

Aerospace Science and Technology

www.elsevier.com/locate/aescte

Guidance law implementation with performance recovery using an extended high-gain observer ☆

Kemao Ma [a,*], Hassan K. Khalil [b], Yu Yao [a]

[a] Control and Simulation Center, School of Astronautics, Harbin Institute of Technology, 150080, China
[b] Department of Electrical and Computer Engineering, Michigan State University, MI 48823, United States

ARTICLE INFO

Article history:
Received 28 January 2009
Received in revised form 24 December 2010
Accepted 3 November 2011
Available online 22 November 2011

Keywords:
Guidance law
Target maneuver
High-gain observer
Performance recovery

ABSTRACT

Guidance law of a homing missile is implemented using an extended high gain observer without the model assumptions on target maneuvers. First, for a class of multi-input–multi-output nonlinear systems, extended high-gain observers are used for output feedback control with partial practical stabilization. Then the method is applied to the guidance law implementation of a homing missile with bearing only measurement. Simulation results show satisfactory performance.

1. Introduction

In the terminal guidance phase of a homing missile with bearing only measurement (BOM) system, as in the case of a homing missile with a passive infrared seeker, only line-of-sight (LOS) angle signals are available for guidance. The widely used Proportional Navigation Guidance (PNG) law, as well as many other improved guidance laws based on PNG, feeds back the LOS rate signals to stabilize the LOS rate. Thus to implement the guidance laws, it is necessary to estimate the differentials of LOS angle signals. Beside the LOS angle and LOS rate signals, modern guidance laws utilize the relative range, relative range rate, and target maneuver signals to cancel out the nonlinearities and compensate for the target maneuvers. Conventional implementation methods include observers and digital filters, both of which require the observability of the signals to be estimated [1–3].

Difficulties arise from the lack of observability of the signals to be estimated. Simple analysis shows that if no additional measurement is available, different ranges and target maneuvers are indistinguishable from the LOS angles [2]. A common approach to tackle this difficulty is to incorporate the target motion dynamics to the guidance model [1]. The guidance performance will be seriously deteriorated if there exists significant difference between the real target maneuver and model prediction.

In this paper, a different idea is proposed. All the signals necessary to the guidance law implementation are estimated using a high gain observer. In the relative motion equations of the missile and its target, the nonlinear terms, consisting of the signals of the LOS rates, relative range and its rate, are treated as model uncertainties, and the target maneuvers are treated as external disturbances. The model uncertainties and external disturbances can be estimated by extending the order of the observer. Using the estimates of the extended observer, the cancellation of nonlinear terms and compensation for target maneuvers in the guidance laws can be implemented. In doing so, the observability assumptions of target maneuver, relative range and relative range rate, required by other methods, are removed, and no target maneuver model is needed for the guidance law implementation.

The use of high-gain observers is a practical approach to implementation of state feedback control of nonlinear systems [4]. A high-gain observer can robustly estimate the derivatives of the output, which are used to replace the true states in state feedback control. The observer state will converge very fast, but with a peaking phenomenon. To protect the state of the system from peaking, the state feedback control is required to be globally bounded. This requirement is usually met by saturating a continuous state feedback function outside a compact region of interest. The theoretical base for the use of high-gain observers in output feedback control is the so-called separation principle. For the closed-loop system of a class of nonlinear systems with output feedback control using high-gain observers, a fairly general separation principle can be guaranteed in the sense that the performance of a globally bounded partial state feedback control can be recovered, and the performance recovery includes asymptotic stability of the origin,

☆ This work was supported in part by the National Natural Science Foundation of China under grant number 61174001. The work of the second author was supported in part by the National Science Foundation under grant number ECCS-0725165.
* Corresponding author.
E-mail address: makemao@hit.edu.cn (K. Ma).

1270-9638/$ – see front matter
doi:10.1016/j.ast.2011.11.005

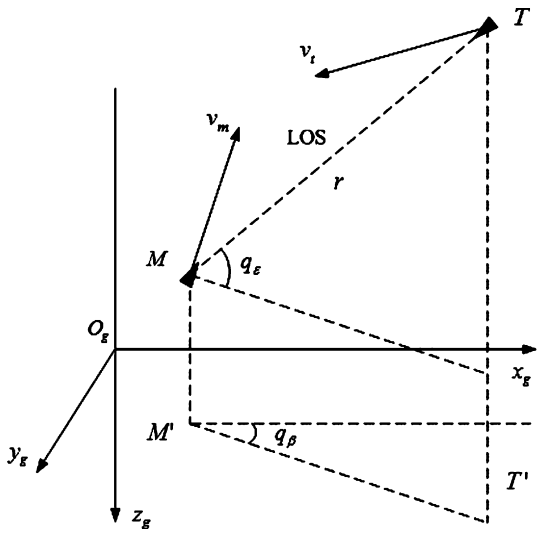

Fig. 1. Three-dimensional attack geometry.

the region of attraction and trajectories [5]. Theoretical investigations and practical applications of high-gain observers include stabilization, nonlinear servomechanisms, adaptive control, sliding mode control, robustness to fast un-modeled dynamics, discrete-time implementation and application to induction motors [6].

Although widely discussed, literature concerning high-gain observer technique includes only the systems whose stability is with respect to all state variables. In [5], asymptotic stability of the origin is discussed. In [7], bounded-input–bounded-state stability is assumed on the zero dynamics. In other cases, similar stability assumptions, such as input-to-state stability, on zero dynamics are required. However, for the guidance problem of a homing missile against a target, only the LOS rate signals, which are only a part of the whole system's state variables, are to be stabilized [8–11]. In many engineering applications, consideration of stability with respect to part of the system's state variables, the so-called partial stability, is also necessary [12,13]. Other examples of partial stability can be found in many fields such as electro-magnetics, inertial navigation systems, spacecraft stabilization via flywheels, biocenology [14].

The rest of the paper is organized as follows. In Section 2, the guidance dynamics of a homing missile are discussed. Section 3 designs an extended observer to recover the performance of a state feedback control law. In Section 4, the extended high-gain observer is used to implement the guidance law of a missile in a terminal guidance phase, and simulation is conducted. We concludes the paper with Section 5.

2. Guidance dynamics of a homing missile

For a homing missile in the terminal guidance phase, the task of guidance laws is to steer the missile to intercept its designated target with a tolerable miss distance. The general three-dimensional attack geometry, in an inertial coordinates frame, is shown in Fig. 1. M and T represent the missile and the target, respectively, both of which are considered as mass points in designing guidance laws. r is the relative range between the missile and the target, and v_m and v_t are velocity vectors of the missile and the target, respectively. The line connecting M and T is LOS, the orientation of which in coordinates frame $O_g x_g y_g z_g$ determines q_β and q_ε, the LOS angles in horizontal and longitudinal planes, respectively.

Three-dimensional relative motion between the missile and its target, as shown in Fig. 1, can be described as follows [18]:

$$\ddot{r} = r\dot{q}_\varepsilon^2 + r\dot{q}_\beta^2 \cos^2 q_\varepsilon \tag{1}$$

$$\ddot{q}_\beta = -\frac{2\dot{r}}{r}\dot{q}_\beta + 2\dot{q}_\varepsilon \dot{q}_\beta \tan q_\varepsilon + \frac{a_{ty} - a_{my}}{r\cos q_\varepsilon} \tag{2}$$

$$\ddot{q}_\varepsilon = -\frac{2\dot{r}}{r}\dot{q}_\varepsilon - \dot{q}_\beta^2 \sin q_\varepsilon \cos q_\beta - \frac{a_{tz} - a_{mz}}{r} \tag{3}$$

where a_{ty} and a_{my} are the acceleration components of the target and the missile in the longitudinal plane, respectively, both perpendicular to the LOS. a_{tz} and a_{mz} are the acceleration components of the target and the missile in the horizontal plane, respectively, both perpendicular to the LOS.

Guidance laws are designed to issue lateral acceleration commands, a_{myc} and a_{mzc}. The autopilot of the missile receives lateral acceleration commands from the guidance system and causes aerodynamic surfaces to move so as to attain these commanded accelerations. In a guidance law design routine, the dynamics of the missile autopilot control loop are often omitted to simplify the design. Thus, we assume

$$a_{my} = a_{myc}, \qquad a_{mz} = a_{mzc}$$

The aerodynamic acceleration capability of a missile is physically limited by such factors as the existence of stall angle of attack, the maximum defection of movable control surfaces. In an actual missile, the airframe acceleration must also be limited in order to prevent structural failure. Thus we have the following constraint

$$|a_{my}| \leqslant a_M, \qquad |a_{mz}| \leqslant a_M \tag{4}$$

where a_M is the maximum aerodynamic acceleration the missile can provide perpendicular to LOS, in both horizontal and vertical planes.

A missile with passive BOM system is considered. The seeker, which has a minimum effective operation range, denoted by r_E, provides the LOS angle measurement for the implementation of guidance law, i.e., only LOS angle signals, q_β and q_ε, are available for guidance laws implementation. In the missile's engagement against the target, if the relative range r is equal to or less than r_E, effective guidance signals are no longer available, and seeker gives a command to stop the guidance. In the remaining time of the engagement, the missile is in a free flight without guidance. Note that the existence of r_E rules out the singularity in the analysis of guidance loop. In the free flight phase, the minimum range of the missile with respect to the target, $r_{\min}$, is the miss distance, a main performance measure to be minimized by guidance law design.

In designing guidance laws, the LOS rates in both horizontal and longitudinal planes, $\dot{q}_\beta$ and $\dot{q}_\varepsilon$, are to be stabilized. In an ideal interception, i.e. when $\dot{q}_\beta = 0$ and $\dot{q}_\varepsilon = 0$, the relative motion equations (1), (2), (3) reduce to

$$\ddot{r} = 0$$

which means that the missile flies directly to the target with a constant relative velocity $\dot{r} < 0$, and a zero miss distance is to be achieved. In an actual engagement, the miss distance, $r_{\min}$, can be achieved to a small required value if the LOS rates are kept small. PNG laws, a widely used class of guidance laws, use feedback control, proportional to the LOS rates, to stabilize the LOS rates. It is shown that a PNG law, with an appropriately selected navigation ratio, is optimal with respect to a quadratic cost, consisting miss distance and lateral accelerations, against a target without maneuver escapes [10]. The guidance performance deteriorates with the presence of target maneuvers [15]. To keep the optimality in a scenario with target maneuvers, the PNG laws must be augmented to include target maneuver compensations. An augmented PNG law takes the following form

$$a_{my} = N_y \dot{q}_\beta r \cos q_\varepsilon + a_{ty} - 2\dot{r}\dot{q}_\beta \cos q_\varepsilon + 2r\dot{q}_\varepsilon \dot{q}_\beta \sin q_\varepsilon \tag{5}$$

$$a_{mz} = -N_z \dot{q}_\varepsilon r + a_{tz} + 2\dot{r}\dot{q}_\varepsilon + r\dot{q}_\beta^2 \sin q_\varepsilon \cos q_\beta \tag{6}$$

where $N_y > 0$ and $N_z > 0$ are constants. The relative motion and the augmented PNG constitute the closed-loop guidance loop. Note that only partial state variables, i.e. $\dot{q}_\beta$ and $\dot{q}_\varepsilon$, are to be stabilized in the guidance loop, and only q_β and q_ε are available from measurement for feedback in (5) and (6). The other signals in (5) and (6), unavailable from measurement, are to be estimated using an extended high-gain observer described in the next section.

3. High-gain observer design and performance recovery

The three-dimensional relative motion dynamics developed in the above section can be formulated as a general multi-input–multi-output nonlinear system in the following normal form

$$\dot{x} = Ax + B\big[b(x,z,d) + a(x,z,d)u\big] \tag{7}$$

$$\dot{z} = f_0(x,z) \tag{8}$$

$$y = Cx \tag{9}$$

$$w = Ex \tag{10}$$

where $x \in \mathbb{R}^\rho$ and $z \in \mathbb{R}^m$ are the state variables, $u \in \mathbb{R}^p$ is the control input, $d \in \mathbb{R}^q$ is a vector of unknown external disturbances, and $y \in \mathbb{R}^p$ is the measured output. The $\rho \times \rho$ matrix A, the $\rho \times p$ matrix B, and the $p \times \rho$ matrix C, given by

$$A = \text{block diag}[A_1, \ldots, A_p], \quad A_i = \begin{bmatrix} 0 & 1 & 0 & \cdots & 0 \\ 0 & 0 & 1 & \cdots & 0 \\ \vdots & \vdots & \ddots & \ddots & \vdots \\ 0 & 0 & \cdots & 0 & 1 \\ 0 & 0 & \cdots & 0 & 0 \end{bmatrix}_{\rho_i \times \rho_i}$$

$$B = \text{block diag}[B_1, \ldots, B_p], \quad B_i = \begin{bmatrix} 0 \\ 0 \\ \vdots \\ 0 \\ 1 \end{bmatrix}_{\rho_i \times 1}$$

$$C = \text{block diag}[C_1, \ldots, C_p], \quad C_i = \begin{bmatrix} 1 & 0 & \cdots & 0 & 0 \end{bmatrix}_{1 \times \rho_i}$$

where $1 \leqslant i \leqslant p$ and $\rho = \rho_1 + \cdots + \rho_p$ represent p chains of integrators. $b(\cdot,\cdot,\cdot)$ and $a(\cdot,\cdot,\cdot)$ are p-dimensional nonlinear function vector and $p \times p$ nonlinear function matrix, respectively. The vector $w \in \mathbb{R}^n$ is a part of the state extracted from x by the selection matrix

$$E = \text{block diag}[E_1, \ldots, E_p]$$

$$E_i = \begin{bmatrix} e_{\rho_i - n_i + 1} & \cdots & e_{\rho_i} \end{bmatrix}^T \in \mathbb{R}^{n_i \times \rho_i}, \quad 1 \leqslant i \leqslant p$$

where $n = n_1 + \cdots + n_p$ and e_i is a vector with all elements being zeros except the ith element being 1. After the extraction, the remained partial state of x is denoted by $\bar{w}$. It is assumed that

Assumption 1. Both $d(t)$ and $\dot{d}(t)$ are bounded and $d(t) \in W \subset \mathbb{R}^q$, where W is a compact set.

Assumption 2. $f_0(\cdot,\cdot)$ is locally Lipschitz and continuous on its domain, and the nonlinear function vector $b(\cdot,\cdot,\cdot)$ and matrix $a(\cdot,\cdot,\cdot)$ are continuously differentiable with locally Lipschitz derivatives. The zero dynamics equation (8) has no finite escape time.

Remark 1. For the system (7)–(10), suppose that only w needs to be stabilized, i.e. only the stability with respect to the set $\{w = 0\}$ is required. For the partial state z, by Assumption 2 it can be shown that for any compact sets $S_z \subset \mathbb{R}^m$, $S_z^0 \subset \mathbb{R}^m$, with S_z^0 in the interior of S_z, and $S_x \subset \mathbb{R}^\rho$ with $S_z \times S_x$ in the domain of $f_0(\cdot,\cdot)$, f_0 is continuous on $S_z \times S_x$, and for any $z(0) \in S_z^0$ and $x(t) \in S_x$, there exists $T > 0$, such that $z(t) \in S_z$, $\forall t \in [0, T]$. This property is less restrictive than various stability assumptions [7,5] which can be viewed as special cases of the property where $T = \infty$. In addition, when T is finite, unstable cases which admit no finite escape times can also be covered by the property.

The goal is to design an output feedback controller to regulate the partial state, w, to zero, for all initial states in a given compact set, while meeting certain requirements on the transient response. For system (7)–(10), if only the selected part of the state, w, is considered, then for the dynamics of w, we have

$$\begin{aligned} \dot{w} &= EAx + EB\big[b(x,z,d) + a(x,z,d)u\big] \\ &= \bar{A}w + \bar{B}\big[b(x,z,d) + a(x,z,d)u\big] \end{aligned} \tag{11}$$

where the $n \times n$ matrix $\bar{A}$ and $n \times p$ matrix $\bar{B}$ are given by

$$\bar{A} = EA = \text{block diag}[\bar{A}_1, \ldots, \bar{A}_p]$$

$$\bar{A}_i = \begin{bmatrix} 0 & 1 & 0 & \cdots & 0 \\ 0 & 0 & 1 & \cdots & 0 \\ \vdots & \vdots & \ddots & \ddots & \vdots \\ 0 & 0 & \cdots & 0 & 1 \\ 0 & 0 & \cdots & 0 & 0 \end{bmatrix}_{n_i \times n_i}$$

$$\bar{B} = EB = \text{block diag}[\bar{B}_1, \ldots, \bar{B}_p], \quad \bar{B}_i = \begin{bmatrix} 0 \\ 0 \\ \vdots \\ 0 \\ 1 \end{bmatrix}_{n_i \times 1}, \ 1 \leqslant i \leqslant p$$

Since Eq. (11) is dependent on $\bar{w}$ and z, Eq. (8) and the dynamics of $\bar{w}$ cannot be dropped out of consideration. Obviously, had (x,z,d) been available for feedback and the functions $a(\cdot,\cdot,\cdot)$ and $b(\cdot,\cdot,\cdot)$ been known, we could have chosen a static control law as the following feedback linearization

$$u = a^{-1}(x,z,d)\big(-b(x,z,d) + v\big) \tag{12}$$

and the dynamics of w would have been reduced to

$$\dot{w} = \bar{A}w + \bar{B}v \tag{13}$$

The auxiliary control v could then be designed, for example, as the linear partial state feedback control $v = -Kw$, where $(\bar{A} - \bar{B}K)$ is Hurwitz and the solution of

$$\dot{w} = (\bar{A} - \bar{B}K)w \tag{14}$$

meets certain transient response requirements. The corresponding x dynamics are

$$\dot{x} = (A - BKE)x \tag{15}$$

By choosing the feedback gain matrix K, the partial state w can be regulated arbitrarily small, i.e. for any $\delta > 0$, there exists certain $T^* > 0$, such that $\|w(t)\| < \delta/2$ for $T^* < t < T$. We call the feedback gain matrix K chosen in this way acceptable. In this case, for the partial stability of w, we could choose $V_w(w) = w^T P_w w$, independent of $\bar{w}$ and z, where $P_w = P_w^T > 0$ is the solution of the Lyapunov equation

$$P_w(\bar{A} - \bar{B}K) + (\bar{A} - \bar{B}K)^T P_w = -Q_w$$

for some $Q_w = Q_w^T > 0$.

Remark 2. For any $c > 0$, the set $\Omega_c = \{V_w(w) \leqslant c\} \times \mathbb{R}^{\rho-n} \times \mathbb{R}^m$ is positively invariant for the closed-loop system. For a given compact set $S_w^0 \times S_{\bar{w}}^0 \times S_z^0 \subset \Omega_c$, if $(w(0), \bar{w}(0), z(0)) \in S_w^0 \times S_{\bar{w}}^0 \times S_z^0$, then by the dependence of $\bar{w}$ on w (see Eq. (7)) and Remark 1, for any $T' < T$, there are compact sets $S'_{\bar{w}}$ and S'_z, dependent on c, T' and $S_w^0 \times S_{\bar{w}}^0 \times S_z^0$, such that $(w, \bar{w}, z) \in \Omega'_c = \{V_w(w) \leqslant c\} \times S_{\bar{w}} \times S_z$ for $0 \leqslant t < T'$. The existence of $S'_{\bar{w}}$ is guaranteed by the fact that the solutions of (15) have no finite escape time.

Only the measured output y is available for feedback. Since (A, C) is observable by definition, x can be estimated using an observer. But if linearization feedback (12) is applied to system (7)–(10), then the partial state z is unobservable from y. So it is impossible to estimate partial state z using an observer. To implement the feedback (12), we use the observer to estimate x, and use the nominal models of $a(\cdot,\cdot,\cdot)$, $b(\cdot,\cdot,\cdot)$ in the control law, then extend the observer to compensate for the errors between nominal models and real functions, including the external disturbance d, as discussed in next section.

The extended high-gain observer, with an additional integrator to each of the p chains of integrators in (7)–(10), has the form

$$\dot{\hat{x}} = A\hat{x} + B\big[\hat{\sigma} + \hat{b}(\hat{x}) + \hat{a}(\hat{x})u\big] + H(\varepsilon)(y - C\hat{x}) \tag{16}$$

$$\dot{\hat{\sigma}} = F(\varepsilon)(y - C\hat{x}) \tag{17}$$

where $\hat{a}(\cdot)$, nonsingular, and $\hat{b}(\cdot)$, are the nominal models of $a(\cdot,\cdot,\cdot)$ and $b(\cdot,\cdot,\cdot)$, and are twice continuously differentiable functions, respectively. The extended observer state $\hat{\sigma} = [\hat{\sigma}_1, \ldots, \hat{\sigma}_p]^T$. The observer gain matrices $H(\varepsilon)$ and $F(\varepsilon)$ are given by

$$H(\varepsilon) = \operatorname{block\,diag}\big[H_1(\varepsilon), \ldots, H_p(\varepsilon)\big]$$

$$H_i(\varepsilon) = \begin{bmatrix} \frac{\alpha_1^i}{\varepsilon} \\ \frac{\alpha_2^i}{\varepsilon^2} \\ \vdots \\ \frac{\alpha_{\rho_i-1}^i}{\varepsilon^{\rho_i-1}} \\ \frac{\alpha_{\rho_i}^i}{\varepsilon^{\rho_i}} \end{bmatrix}_{\rho_i \times 1}, \quad i = 1, \ldots, p$$

$$F(\varepsilon) = \operatorname{diag}\left[\frac{\alpha_{\rho_1+1}^1}{\varepsilon^{\rho_1+1}}, \ldots, \frac{\alpha_{\rho_p+1}^p}{\varepsilon^{\rho_p+1}}\right]$$

where $\alpha_1^i, \ldots, \alpha_{\rho_i}^i, \alpha_{\rho_i+1}^i$, $i = 1, \ldots, p$, are real numbers and such chosen that all the polynomials

$$s^{\rho_i+1} + \alpha_1^i s^{\rho_i} + \cdots + \alpha_{\rho_i}^i s + \alpha_{\rho_i+1}^i, \quad i = 1, \ldots, p$$

are Hurwitz, and $\varepsilon > 0$ is a small design parameter. For the function matrix $\hat{a}(\cdot)$, it is assumed.

Assumption 3. For all $(w, \bar{w}, z) \in \Omega'_c$ and $d \in W$, there exists a constant K_a, $0 < K_a < 1$, such that

$$\big\|\big(a(x,z,d) - \hat{a}(x)\big)\hat{a}^{-1}(x)\big\| \leqslant K_a$$

Remark 3. By continuity, all the elements of $a(x,z,d)$ are bounded over the compact set $\Omega'_c \times W$. For $p = 1$, the assumption can always be satisfied, as shown in [7]. For $p > 1$, in the special case where $a(x,z,d)$ is diagonal, if all the upper bounds of $|a_{ii}(x,z,d)|$, $i = 1, \ldots, p$, are known, then Assumption 3 can also be satisfied by choosing

$$\operatorname{sign}\big(\hat{a}_{ii}(x)\big) = \operatorname{sign}\big(a_{ii}(x,z,d)\big)$$

$$\big|\hat{a}_{ii}(x)\big| > \max_{(x,z,d)\in\Omega'_c\times W}\big\{\big|a_{ii}(x,z,d)\big|\big\}, \quad i = 1, \ldots, p$$

Similar conclusion can be drawn in the case where $a(x,z,d)$ is diagonally predominant for all $(x,z,d) \in \Omega'_c \times W$. In other cases, it must be checked if there are nominal models or not such that the assumption is satisfied for the given systems.

It can be anticipated that the term $H(\varepsilon)(y - C\hat{x})$ will be $O(\varepsilon)$ after a short transient period, thus Eq. (16) can be regarded as a perturbation of

$$\dot{\hat{x}} = A\hat{x} + B\big[\hat{\sigma} + \hat{b}(\hat{x}) + \hat{a}(\hat{x})u\big]$$

Multiplying both sides by E, we have

$$\dot{\hat{w}} = \bar{A}\hat{w} + \bar{B}\big[\hat{\sigma} + \hat{b}(\hat{x}) + \hat{a}(\hat{x})u\big] \tag{18}$$

Then the following controller

$$u = \hat{a}^{-1}(\hat{x})\big(-\hat{\sigma} - \hat{b}(\hat{x}) - K\hat{w}\big) = \psi(\hat{x}, \hat{\sigma}) \tag{19}$$

where $\hat{w} = E\hat{x}$, will make (18) coincide with (14). To protect the system from peaking in the observer's transient response, as conventionally done in output feedback control using high-gain observers, the control should be saturated outside the region of interest, i.e. the compact set in which the state variables are contained in the interval $[0, T]$. For notation convenience, denote $\hat{a}^{-1}(\hat{x})$ and $a^{-1}(x,z,d)$ by $\bar{\hat{a}}(\hat{x})$ and $\bar{a}(x,z,d)$, respectively, and let

$$M_i > \max_{(x,z)\in S_x\times S_z, d\in W}\left|\sum_{j=1}^{p}\bar{a}_{ij}(x,z,d)\big(-b_j(x,z,d) + v_j\big)\right|$$
$$i = 1, \ldots, p \tag{20}$$

where $v = [v_1, \ldots, v_p]^T = -Kw$. Using the standard saturation function sat [4–6], we saturate the control (19) as follows

$$u = \bar{M}\operatorname{sat}\big(\bar{M}^{-1}\psi(\hat{x}, \hat{\sigma})\big) = \begin{bmatrix} M_1 \min\{1, |\psi_1(\hat{x},\hat{\sigma})|/M_1\}\operatorname{sign}(\psi_1(\hat{x},\hat{\sigma})) \\ \vdots \\ M_p \min\{1, |\psi_p(\hat{x},\hat{\sigma})|/M_p\}\operatorname{sign}(\psi_p(\hat{x},\hat{\sigma})) \end{bmatrix} \tag{21}$$

where $\bar{M} = \operatorname{diag}[M_1, \ldots, M_p]$.

Let

$$G(s) = \operatorname{diag}\big[G_1(s), \ldots, G_p(s)\big]$$

$$G_i(s) = \frac{\alpha_{\rho_i+1}^i}{(s)^{\rho_i+1} + \alpha_1^i(s)^{\rho_i} + \cdots + \alpha_{\rho_i+1}^i}, \quad i = 1, \ldots, p$$

By the diagonal structure of $G(s)$ we have properties similar to scalar case discussed in [7]:

$$\big\|G(s)\big\|_\infty \triangleq \max_{1<i\leqslant p}\sup_{\omega}\big|G_i(j\omega)\big| \geqslant 1$$

and when poles of each $G_i(s)$ are assigned to be real by appropriately choosing the design parameters α_j^i, we have $\|G(s)\|_\infty = 1$.

Denote the solutions of (14) and (15) by $w^*(t)$ and $x^*(t)$, respectively, and we have the following theorem.

Theorem 1. *For the closed-loop system (7)–(10), (16)–(17) and (21) with an acceptable K and Assumptions 1 to 3 satisfied, if*

$$\big\|G(\varepsilon s)\big\|_\infty K_a < 1 \tag{22}$$

then with bounded observer initial state and each $(w(0), \bar{w}(0), z(0)) \in S_w^0 \times S_{\bar{w}}^0 \times S_z^0$, for any $\delta > 0$, there exist $T^* \in (0, T)$ and $\bar{\varepsilon} > 0$ such that for each $\varepsilon \in (0, \bar{\varepsilon})$:

$$\left\|x(t)-x^*(t)\right\| \to 0 \quad as\ \varepsilon \to 0,\ uniformly\ in\ t,$$
$$for\ t \in [0,T]\ with\ x(0)=x^*(0)$$
$$\left\|w(t)\right\| < \delta, \quad for\ T^* < t < T$$

The proof of the theorem is given in Appendix A.

Remark 4. Better performance recovery can be achieved with the decrease of ε. As pointed out in [5], the high-gain observer, in essence, estimates the derivatives of the state. Thus as shown in [17], with the presence of measurement noise, the value of ε suitable for practical use is bounded from below due to the noise amplification effect of high-gain observer. Considering the measurement noise, the output of the system (9) becomes

$$y = Cx + n_s \tag{23}$$

where $n_s \in \mathbb{R}^p$ is the measurement noise vector, bounded with $\|n_s(t)\| \leqslant \mu$. In such a case, the estimation error satisfies the ultimate bound

$$\left\|x(t)-\hat{x}(t)\right\| \leqslant \varepsilon c_1 + \frac{\mu}{\varepsilon^{r-1}}c_2 \tag{24}$$

for some positive constants c_1 and c_2. Since the estimation error is of the order of magnitude $O(1/\varepsilon^{r-1})$, too small ε deteriorates the estimation performance. A tradeoff must be considered between noise amplification and performance recovery including the state reconstruction speed and uncertainties estimation. The inequality (24) shows that the lower bound on ε is of the order of magnitude $O(\mu^{1/r})$. A switched-gain observer scheme is proposed to relax the tradeoff in [17], to which the interested reader is referred for details.

4. Guidance law implementation using an extended high-gain observer

4.1. High-gain observer design and guidance law implementation

Take

$$x = \begin{bmatrix} x_1 \\ x_2 \\ x_3 \\ x_4 \end{bmatrix} = \begin{bmatrix} q_\beta \\ \dot{q}_\beta \\ q_\varepsilon \\ \dot{q}_\varepsilon \end{bmatrix}, \qquad w = \begin{bmatrix} x_2 \\ x_4 \end{bmatrix} = \begin{bmatrix} \dot{q}_\beta \\ \dot{q}_\varepsilon \end{bmatrix}$$
$$\bar{w} = \begin{bmatrix} x_1 \\ x_3 \end{bmatrix} = \begin{bmatrix} q_\beta \\ q_\varepsilon \end{bmatrix}, \qquad z = \begin{bmatrix} z_1 \\ z_2 \end{bmatrix} = \begin{bmatrix} r \\ \dot{r} \end{bmatrix}$$
$$u = \begin{bmatrix} u_1 \\ u_2 \end{bmatrix} = \begin{bmatrix} a_{my} \\ a_{mz} \end{bmatrix}, \qquad d = \begin{bmatrix} d_1 \\ d_2 \end{bmatrix} = \begin{bmatrix} a_{ty} \\ a_{tz} \end{bmatrix}$$

and the relative motion, shown by Eqs. (1), (2) and (3), writes in the form of (7)–(10), where $p=2$, $\rho=4$, $n=2$, $m=2$, and

$$b(x,z,d) = \begin{bmatrix} b_1(x,z,d) \\ b_2(x,z,d) \end{bmatrix} = \begin{bmatrix} -\frac{2z_2}{z_1}x_2 + 2x_4x_2\tan x_3 + \frac{d_1}{z_1\cos x_3} \\ -\frac{2z_2}{z_1}x_4 - x_2^2\sin x_3\cos x_1 - \frac{d_2}{z_1} \end{bmatrix} \tag{25}$$

$$a(x,z,d) = \begin{bmatrix} -\frac{1}{z_1\cos x_3} & 0 \\ 0 & \frac{1}{z_1} \end{bmatrix} \tag{26}$$

$$f_0(x,z) = \begin{bmatrix} z_2 \\ z_1x_3^2 + z_1x_2^2\cos^2 x_3 \end{bmatrix} \tag{27}$$

Due to the existence of the effective operation range of the seeker r_E, in the guided flight phase of the missile, we have $z_1(t) \geqslant r_E$, thus $a(\cdot,\cdot,\cdot)$ is invertible and bounded provided x_3 remains small. By the continuity and magnitude limitation of target maneuvers, Assumption 1 is satisfied. Applying the guidance laws (5) and (6) to the relative motion equations (1)–(3), $\dot{q}_\beta$ and $\dot{q}_\varepsilon$ are stabilized and therefore x is restricted in a compact set, denoted by S_x for $t \in [0,T]$. For $x \in S_x$ we can give the description of set S_z as follows

$$r_m \leqslant r \leqslant r_M, \quad 0 < r_m < r_E$$
$$\dot{r}_m \leqslant \dot{r} \leqslant \dot{r}_M, \quad \dot{r}_M < 0$$

where $r_m, r_M, \dot{r}_m, \dot{r}_M$ are parameters to describe all the possible engagement scenarios of the terminal guidance. Denote by T the first time when z goes out of S_z, then for any $t \in [0,T]$, $z(t) \in S_z$. Since $\dot{r}$ has little change during the terminal guidance phase and $r_E > r_m$, so we can appropriately choose $\dot{r}_m, \dot{r}_M$ such that there exists a finite $\bar{T} < T$ given by $r(\bar{T}) = r_E$.

In the state space description of the relative motion, target maneuver components, $d_1 = a_{ty}$ and $d_2 = a_{tz}$, are thought of as unknown external disturbances, and terms consisting of state z are thought of as nominal models with uncertain model perturbations, and both uncertainties are included in the nonlinear terms $b(\cdot,\cdot,\cdot)$ and $a(\cdot,\cdot,\cdot)$. For this nonlinear system, we can design an extended high-gain observer as follows

$$\dot{\hat{x}} = A\hat{x} + B\left[\hat{\sigma} + \hat{b}(\hat{x}) + \hat{a}(\hat{x})u\right] + H(\varepsilon)(y - C\hat{x}) \tag{28}$$
$$\dot{\hat{\sigma}} = F(\varepsilon)(y - C\hat{x}) \tag{29}$$

where $\hat{x} \in \mathbb{R}^4$ is the observer state vector, nominal models of $b(\cdot,\cdot,\cdot)$ and $a(\cdot,\cdot,\cdot)$,

$$\hat{b}(\hat{x}) = \begin{bmatrix} \hat{b}_1(\hat{x}) \\ \hat{b}_2(\hat{x}) \end{bmatrix}, \qquad \hat{a}(\hat{x}) = \begin{bmatrix} \hat{a}_1(\hat{x}) & 0 \\ 0 & \hat{a}_2(\hat{x}) \end{bmatrix}$$

are twice continuously differentiable, $\hat{\sigma} = [\hat{\sigma_1}\ \hat{\sigma_2}]^T$ is the extended observer state vector, used to estimate the uncertainties including both model perturbations and disturbances, and the observer gain matrices take the form

$$H(\varepsilon) = \begin{bmatrix} \frac{\alpha_1^1}{\varepsilon} & 0 \\ \frac{\alpha_2^1}{\varepsilon^2} & 0 \\ 0 & \frac{\alpha_1^2}{\varepsilon} \\ 0 & \frac{\alpha_2^2}{\varepsilon^2} \end{bmatrix}, \qquad F(\varepsilon) = \begin{bmatrix} \frac{\alpha_3^1}{\varepsilon^3} & 0 \\ 0 & \frac{\alpha_3^2}{\varepsilon^3} \end{bmatrix}$$

Real numbers α_i^j, $i=1,2,3$, $j=1,2$, are chosen such that both polynomials

$$s^3 + \alpha_1^j s^2 + \alpha_2^j s + \alpha_3^j, \quad j=1,2 \tag{30}$$

are Hurwitz, and different values of $\varepsilon > 0$ will be chosen in the simulation to compare the effects of state observation and performance recovery.

Now we use the estimates of the high-gain observer to implement the guidance laws (5) and (6). For the nonlinearities $b(\cdot,\cdot,\cdot)$ and $a(\cdot,\cdot,\cdot)$ in (25) and (26), state variable z_1 is replaced by r_E, z_2 is replaced by a design parameter $V_c < 0$ according to the typical engagement scenarios the missile is designed to apply. As a result, the nominal models $\hat{b}(\cdot)$ and $\hat{a}(\cdot)$ are as follows

$$\hat{b}(x) = \begin{bmatrix} -\frac{2V_c}{r_E}x_2 + 2x_4x_2\tan x_3 \\ -\frac{2V_c}{r_E}x_4 - x_2^2\sin x_3\cos x_1 \end{bmatrix}$$
$$\hat{a}(x) = \begin{bmatrix} -\frac{1}{r_E\cos x_3} & 0 \\ 0 & \frac{1}{r_E} \end{bmatrix}$$

The model perturbations $b(\cdot,\cdot,\cdot)-\hat{b}(\cdot)$, with external disturbances d_1 and d_2 included, and $a(\cdot,\cdot,\cdot)-\hat{a}(\cdot)$, are compensated for with $\hat{\sigma}$. In the guidance process, $\dot{r}<0$ and T is given implicitly by $r(T)=r_m$. Simple calculation can show that Assumption 3 is satisfied, with $K_a=1-r_m/r_M<1$. When parameters α_j^i, $i=1,2$, $j=1,2,3$, are such chosen that $\|G(s)\|_\infty=1$, the condition (22) is satisfied. Thus, we have the implementation of augmented PNG laws (5) and (6) as follows

$$u_1=N_y\hat{x}_2 r_E\cos\hat{x}_3-2V_c\hat{x}_2\cos\hat{x}_3+2r_E\hat{x}_4\hat{x}_2\sin\hat{x}_3+r_E\hat{\sigma}_1\cos\hat{x}_3 \tag{31}$$

$$u_2=-N_z\hat{x}_4 r_E+2V_c\hat{x}_4+r_E\hat{x}_2^2\sin\hat{x}_3\cos\hat{x}_1-r_E\hat{\sigma}_2 \tag{32}$$

which are saturated as (21) with $M_1=M_2=a_M$.

4.2. Simulations

To compare the performance recovery of guidance law implementation using the designed high-gain observer, the following cases are studied in the simulations:

Case 1. The augmented PNG laws, (5) and (6) using state feedback directly and assuming the target maneuvers a_{my} and a_{mz} to be known.

Case 2. The augmented PNG laws, (31) and (32) implemented with a high-gain observer.

Case 3. The augmented PNG laws, (31) and (32) implemented with a high-gain observer based on an output with measurement noise (23).

Under PNG and augmented PNG laws, homing missiles can conduct interception in any direction with respect to their targets [19, 20]. So in the simulation we choose an engagement scenario with the following initial values and target maneuvers

$$r(0)=5000\text{ m},\qquad \dot{r}(0)=-500\text{ m/s},\qquad q_\beta(0)=20^\circ$$

$$\dot{q}_\beta(0)=0.57^\circ/\text{s},\qquad q_\varepsilon(0)=30^\circ,\qquad \dot{q}_\varepsilon(0)=2.87^\circ/\text{s}$$

$$a_{ty}=40\sin\left(\frac{2\pi}{4}t+\frac{\pi}{4}\right)\text{m/s}^2,\qquad a_{tz}=40\sin\left(\frac{2\pi}{4}t\right)\text{m/s}^2$$

We assume that the missile is equipped with a BOM measurement system, and the effective operation range of the seeker is assumed to be $r_E=150$ m, the maximum aerodynamic acceleration the missile can provide is assumed to be $a_M=400\text{ m/s}^2$. The design parameters of augmented PNG laws are chosen as $N_y=N_z=5$, the design parameter V_c is chosen as $V_c=-550$ m/s.

In the simulations for all Cases 1 through 3, we set $u_1=0$ and $u_2=0$ when $z_1(t)\leqslant r_E$. In Case 1, the miss distance is $r_{\min}=1.30$ m. In Case 2, we first choose $\varepsilon=0.02$, and the corresponding miss distance is $r_{\min}=1.49$ m, similar to that in Case 1. The LOS rates $x_2=\dot{q}_\beta$, $x_4=\dot{q}_\varepsilon$, and their estimates $\hat{x}_2$, $\hat{x}_4$, are shown in Figs. 2 and 3, respectively.

From Figs. 2 and 3, we can see that the LOS rate estimates converge rapidly to the real LOS rate signals, and simulation with other values of ε also shows the smaller the ε, the faster the convergence. The results for other values of ε are omitted. In the simulation results, we can also find the peaking of the observer state, which is a feature of high-gain observers, and the smaller the ε, the larger the peaking. But the boundedness of the nominal models and saturation of control protect the state of the system from peaking.

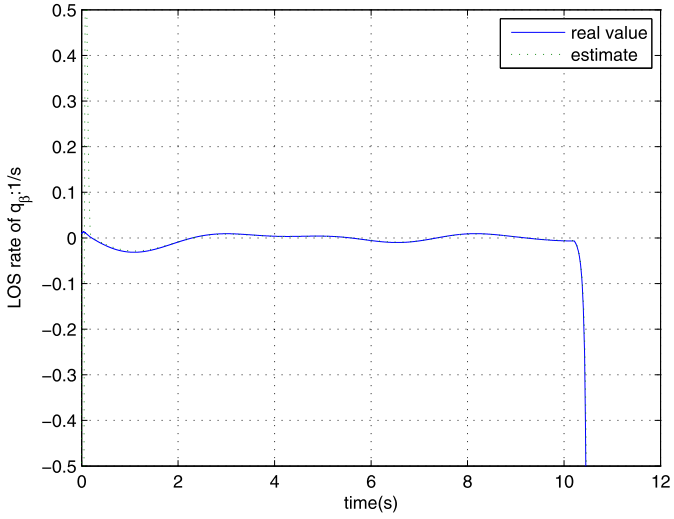

Fig. 2. LOS rate estimation: $\dot{q}_\beta$.

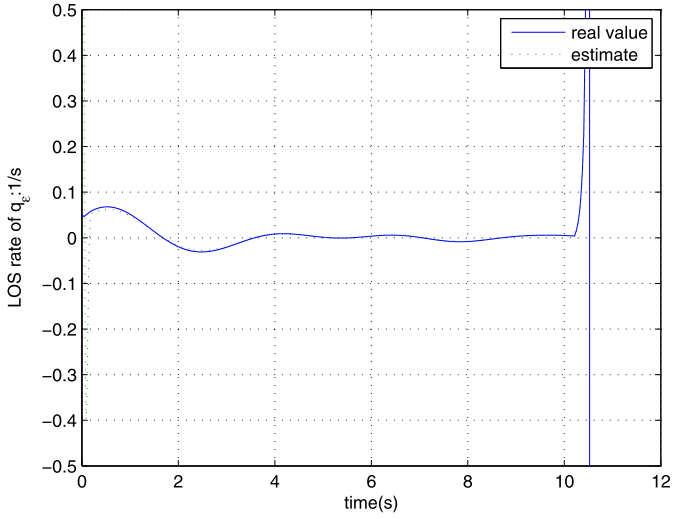

Fig. 3. LOS rate estimation: $\dot{q}_\varepsilon$.

To see the performance recovery of the high-gain observer, we set $\varepsilon=0.002$, and compare a_{my} and a_{mz} at different values of ε in Case 2 and those in Case 1, as shown in Figs. 4 and 5. It can be seen that with the decrease of the value of ε, the acceleration commands implemented with high-gain observers converge to those using direct state feedback with a_{my} and a_{mz} known. This phenomenon is consistent with the dependence of the LOS rate convergence on the value of ε, as discussed above. When $\varepsilon=0.002$, the LOS rate signals, $\dot{q}_\beta$, $\dot{q}_\varepsilon$, are shown in Figs. 6 and 7.

In Case 3, both components of the measurement noise are assumed to be uniformly distributed random variables taking values between -0.6 mrad and 0.6 mrad, and they change values every 0.0002 s. When $\varepsilon=0.02$, the miss distance is $r_{\min}=1.50$ m, little larger than that in Case 3 with the same value of ε, which means that for the high-gain observer, the chosen ε achieves a satisfactory tradeoff between performance recovery and noise amplification. For larger or smaller values of ε, the miss distance increases due to the bad estimation or noise amplification. The real LOS rate signals and their estimates are shown in Figs. 8 and 9, and the acceleration commands are shown in Fig. 10.

It is worth noting that with the presence of measurement noise, different magnitudes of measurement noise signals decide different values that ε takes to achieve an optimal tradeoff between performance recovery and noise amplification, but the statistics of

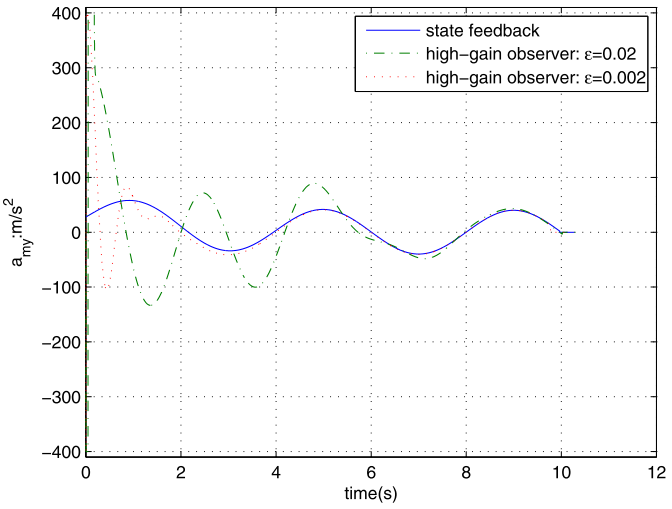

Fig. 4. Performance recovery of a_{my}.

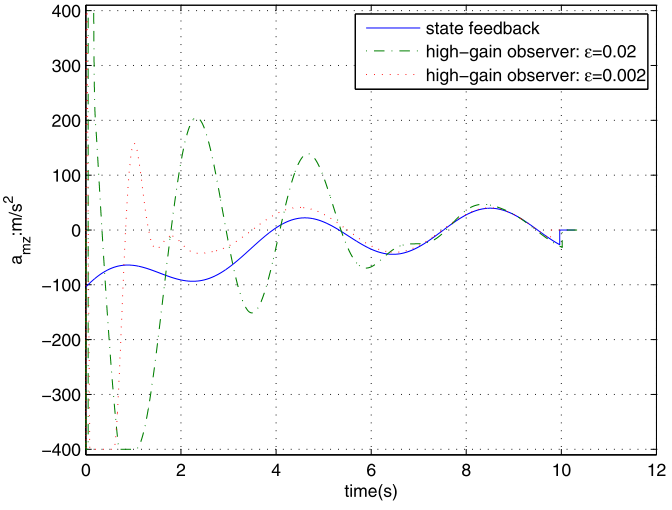

Fig. 5. Performance recovery of a_{mz}.

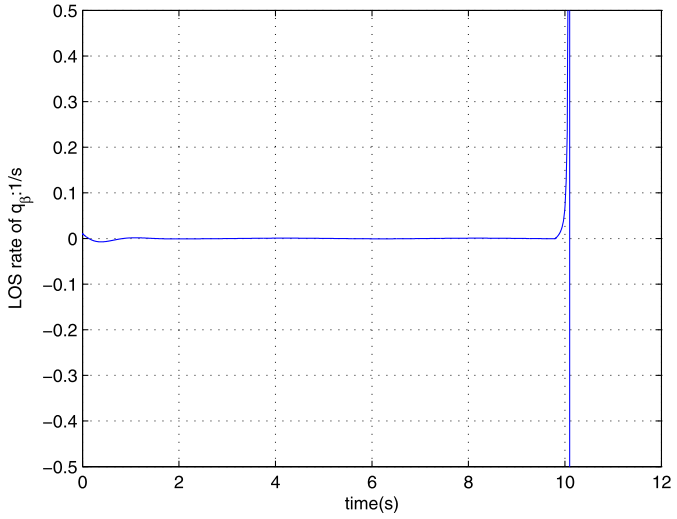

Fig. 6. LOS rate: $\dot{q}_\beta$.

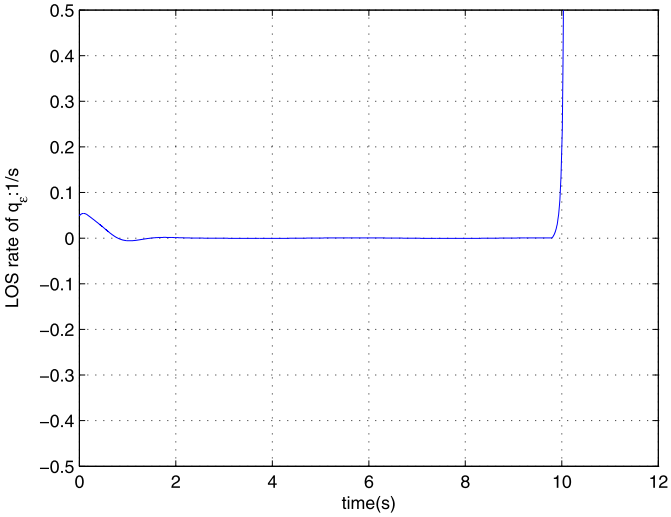

Fig. 7. LOS rate: $\dot{q}_\varepsilon$.

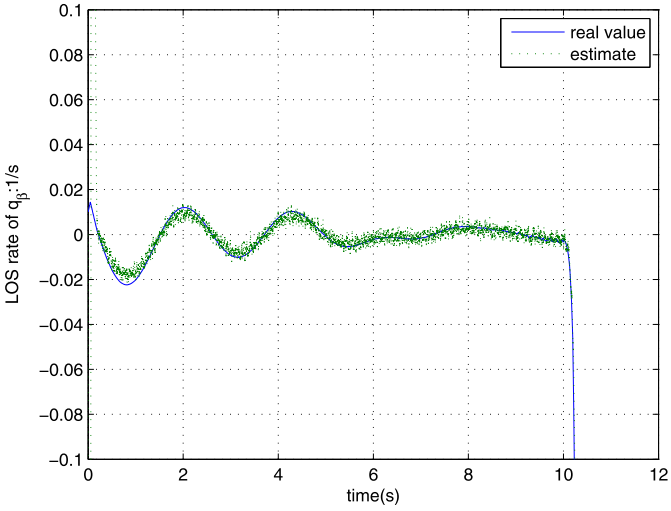

Fig. 8. LOS rate estimation with noise: $\dot{q}_\beta$.

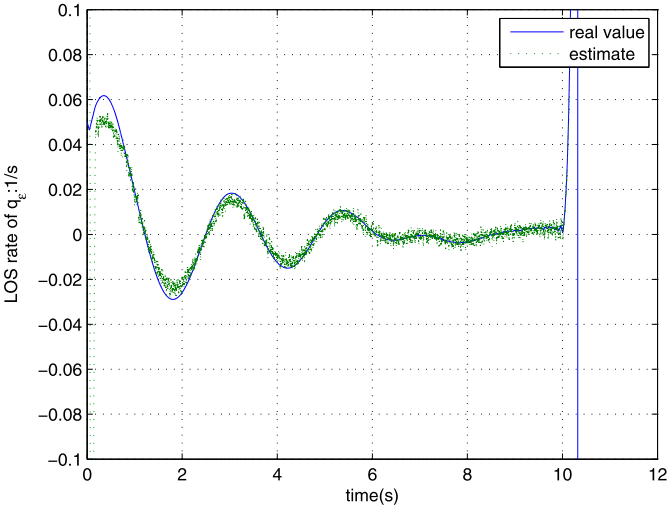

Fig. 9. LOS rate estimation with noise: $\dot{q}_\varepsilon$.

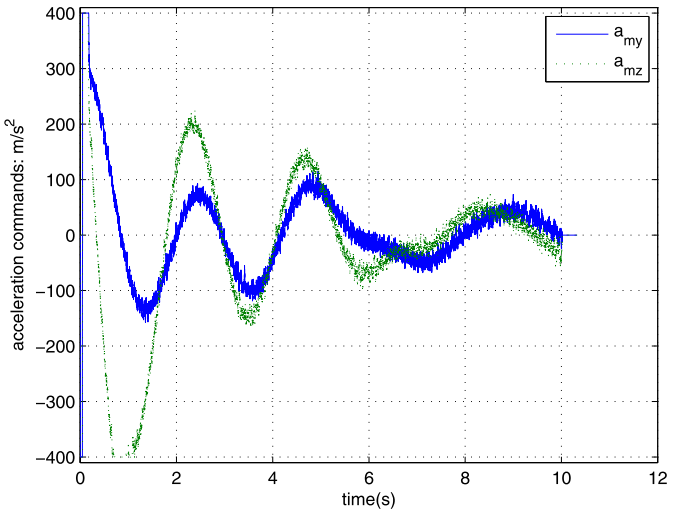

Fig. 10. Acceleration commands with noise.

measurement noise are not necessary to the high-gain observer design, which is different from the filtering method, for which imprecise knowledge of the measurement noise statistics seriously deteriorates the estimation, even results in instability. Also note that in both Cases 2 and 3, no a priori model assumptions are made on target maneuvers, although the target maneuvers are unobservable from the BOM measurement. While for filtering method, either the target maneuver models are assumed [1], or guidance laws are adapted to improve observability [2].

5. Conclusions

For a class of multi-input–multi-output nonlinear systems, extended high-gain observers are used in the output feedback control design. Motivated by the guidance of a homing missile, partial practical stabilization is considered for the class of systems. Since only a part of state variables are practically stabilized, no non-minimum phase conditions are required, unlike the common cases where stabilization of full state is considered. So systems with unstable zero dynamics can also be included in this paper, only if they admit no finite escape times.

As done in [7], the high-gain observer is extended to estimate the perturbation due to model uncertainty and disturbance. The performance recovery is proved.

Then, the extended high-gain observer is applied to the guidance law implementation of a homing missile with bearing only measurement. Simulation results show the satisfactory performance recovery of the extended high-gain observer.

Appendix A. Proof of Theorem 1

Fast variables are scaled estimation errors defined as follows

$$\eta_{ij} = \frac{x_{ij} - \hat{x}_{ij}}{\varepsilon^{\rho_i+1-j}}, \quad 1 \leqslant i \leqslant p,\ 1 \leqslant j \leqslant \rho_i \tag{33}$$

$$\eta_{i(\rho_i+1)} = \Delta_i^b(x,z,d) + \sum_{k=1}^{p} \Delta_{ik}^a(x,z,d) M_k g_\varepsilon\big(\psi_k(x,\hat{\sigma})/M_k\big) - \hat{\sigma}_i$$
$$1 \leqslant i \leqslant p \tag{34}$$

where

$$\Delta_i^b(x,z,d) = b_i(x,z,d) - \hat{b}_i(x)$$
$$\Delta_{ik}^a(x,z,d) = a_{ik}(x,z,d) - \hat{a}_{ik}(x), \quad 1 \leqslant i,k \leqslant p$$

and the odd function $g_\varepsilon(\cdot)$ is defined by [7]

$$g_\varepsilon(y) = \begin{cases} y & \text{for } 0 \leqslant y \leqslant 1 \\ y + (y-1)/\varepsilon - 0.5(y^2-1)/\varepsilon & \text{for } 1 \leqslant y \leqslant 1+\varepsilon \\ 1 + 0.5\varepsilon & \text{for } y \geqslant 1+\varepsilon \end{cases}$$

Since the function g_ε is continuously differentiable, and

$$\frac{\partial}{\partial\hat{\sigma}} \begin{bmatrix} \eta_{1(\rho_1+1)} \\ \vdots \\ \eta_{p(\rho_p+1)} \end{bmatrix} = -I - \Delta^a(x,z,d) \times \operatorname{diag}\big[g_\varepsilon'\big(\psi_1(x,\hat{\sigma})/M_1\big), \ldots, g_\varepsilon'\big(\psi_p(x,\hat{\sigma})/M_p\big)\big]\hat{a}^{-1}(x)$$

It is easy to show that $|g_\varepsilon'(y)| \leqslant 1$ for any $y \in \mathbb{R}$, then in view of Assumption 3, we can see that the change of variable (34) is globally well defined.

The state equations of the fast variables are

$$\varepsilon\dot{\eta}_{ij} = -\alpha_j^i \eta_{i1} + \eta_{i(j+1)}, \quad 1 \leqslant j \leqslant \rho_i - 1$$
$$\varepsilon\dot{\eta}_{i\rho_i} = -\alpha_{\rho_i}^i \eta_{i1} + \eta_{i(\rho_i+1)} + \Delta_i^0(x,z,\hat{x},\hat{\sigma},d,\varepsilon)$$
$$\varepsilon\dot{\eta}_{i(\rho_i+1)} = -\alpha_{\rho_i+1}^i \eta_{i1} - \sum_{k=1}^{p} \Delta_{ik}^a(x,z,d) g_\varepsilon'\big(\psi_k(x,\hat{\sigma})/M_k\big) \times \sum_{l=1}^{p} \bar{\hat{a}}_{kl}(x)\alpha_{\rho_l+1}^l \eta_{l1} + \varepsilon\Bigg[\dot{\Delta}_i^b(x,z,d) + \sum_{k=1}^{p} \dot{\Delta}_{ik}^a(x,z,d) M_k g_\varepsilon\big(\psi_k(x,\hat{\sigma})/M_k\big) + \sum_{k=1}^{p} \Delta_{ik}^a(x,z,d) g_\varepsilon'\big(\psi_k(x,\hat{\sigma})/M_k\big) \frac{\partial\psi_k(x,\hat{\sigma})}{\partial x}\dot{x}\Bigg]$$

for $1 \leqslant i \leqslant p$, where

$$\Delta_i^0(x,z,\hat{x},\hat{\sigma},d,\varepsilon) = \hat{b}_i(x) - \hat{b}_i(\hat{x}) + \sum_{k=1}^{p} a_{ik}(x,z,d) M_k\big[g_\varepsilon\big(\psi_k(\hat{x},\hat{\sigma})/M_k\big) - g_\varepsilon\big(\psi_k(x,\hat{\sigma})/M_k\big)\big] + \sum_{k=1}^{p}\big[\hat{a}_{ik}(x) M_k g_\varepsilon\big(\psi_k(x,\hat{\sigma})/M_k\big) - \hat{a}_{ik}(\hat{x}) M_k g_\varepsilon\big(\psi_k(\hat{x},\hat{\sigma})/M_k\big)\big] + \sum_{k=1}^{p}\big[a(x,z,d) - \hat{a}(\hat{x})\big] M_k\big[\operatorname{sat}\big(\psi_k(\hat{x},\hat{\sigma})/M_k\big) - g_\varepsilon\big(\psi_k(\hat{x},\hat{\sigma})/M_k\big)\big]$$

The fast subsystem is given by

$$\varepsilon\dot{\eta} = \Lambda\eta - \tilde{B}_1\Delta_1 \begin{bmatrix} \alpha_{\rho_1+1}^1 \eta_{11} \\ \vdots \\ \alpha_{\rho_p+1}^p \eta_{p1} \end{bmatrix} + \varepsilon[\tilde{B}_1\Delta_2 + \tilde{B}_2\Delta_3] \tag{35}$$

where

$$\Lambda = \operatorname{block\,diag}[\Lambda_1, \ldots, \Lambda_p], \quad \Lambda_i = \begin{bmatrix} -\alpha_1^i & 1 & 0 & \cdots & 0 \\ -\alpha_2^i & 0 & 1 & \cdots & 0 \\ \vdots & \vdots & \ddots & \ddots & \vdots \\ -\alpha_{\rho_i}^i & 0 & \cdots & 0 & 1 \\ -\alpha_{\rho_i+1}^i & 0 & \cdots & \cdots & 0 \end{bmatrix}$$

$$\tilde{B}_1 = \operatorname{block\,diag}\left[\begin{bmatrix} 0 \\ B_1 \end{bmatrix}, \ldots, \begin{bmatrix} 0 \\ B_p \end{bmatrix}\right]$$

$$\tilde{B}_2 = \operatorname{block\,diag}\left[\begin{bmatrix} B_1 \\ 0 \end{bmatrix}, \ldots, \begin{bmatrix} B_p \\ 0 \end{bmatrix}\right]$$

$$\Delta_1 = \Delta^a(x,z,d) \times \operatorname{diag}\left[g_\varepsilon'\left(\psi_1(x,\hat{\sigma})/M_1\right), \ldots, g_\varepsilon'\left(\psi_p(x,\hat{\sigma})/M_p\right)\right]\hat{a}^{-1}(x)$$

$$\Delta_2 = \dot{\Delta}^b(x,z,d) + \dot{\Delta}^a(x,z,d)\bar{M}\begin{bmatrix} g_\varepsilon(\psi_1(x,\hat{\sigma})/M_1) \\ \vdots \\ g_\varepsilon(\psi_p(x,\hat{\sigma})/M_1) \end{bmatrix} + \Delta^a(x,z,d)\begin{bmatrix} g_\varepsilon'(\psi_1(x,\hat{\sigma})/M_1)\frac{\partial\psi_1(x,\hat{\sigma})}{\partial x}\dot{x} \\ \vdots \\ g_\varepsilon'(\psi_p(x,\hat{\sigma})/M_1)\frac{\partial\psi_p(x,\hat{\sigma})}{\partial x}\dot{x} \end{bmatrix}$$

$$\Delta_3 = \frac{1}{\varepsilon}\Delta_0(x,z,\hat{x},\hat{\sigma},d,\varepsilon)$$

By Assumption 3 and the property that $|g_\varepsilon'(y)| \leqslant 1$, we can show that $\|\Delta_1\| \leqslant 1$. By the definition of variable change (33) and the definition of function g_ε, we can show that Δ_0/ε is locally Lipschitz. Assumption 2 ensures that Δ_2 and Δ_3 are locally Lipschitz and, for $(x,z) \in \Omega_c'$, bounded from above by affine in $\|\eta\|$, uniformly in ε. Let

$$\tilde{C} = \operatorname{block\,diag}\left[\alpha_{\rho_1+1}^1 C_1, \ldots, \alpha_{\rho_p+1}^p C_p\right]$$

and without considering the term $\varepsilon[\tilde{B}_1\Delta_2 + \tilde{B}_2\Delta_3]$, we first consider the following system

$$\varepsilon\dot{\eta} = \Lambda\eta - \tilde{B}_1\Delta_1\tilde{C}\eta \tag{36}$$

The system can be viewed as a negative feedback connection of a linear system and nonlinear gain Δ_1, where the transfer function matrix of the linear system, $\tilde{C}((\varepsilon s)I - \Lambda)^{-1}\tilde{B}_1$, is $G(\varepsilon s)$, which is strictly proper. By Assumption 3, it can be proved that if $\|G(s)\|_\infty < K_a^{-1}$, then $[I + K_a G(\varepsilon s)][I - K_a G(\varepsilon s)]^{-1}$ is strictly positive real, for the details of the proof, see Example 7.1 in [16]. Then according to the circle criterion of absolute stability, it can be shown that the system (36) will be globally exponentially stable, and has a quadratic Lyapunov function $W(\eta) = \eta^T P\eta$. Using $W(\eta)$ as a Lyapunov function candidate for (35), we can conclude that for any $c_1 > 0$, η enters $\{W(\eta) \leqslant \varepsilon^2 c_1\}$ in finite time $T_1(\varepsilon)$, where $\lim_{\varepsilon\to 0} T_1(\varepsilon) = 0$. Since the control is saturated by (21), the right-hand side of (7) is bounded in $[0, T_1(\varepsilon)]$ uniformly in ε, thus if ε is small enough such that $T_1(\varepsilon) < T'$ we have $(w(t), \bar{w}(t), z(t)) \in \Omega_c'$ for $t \in [0, T_1(\varepsilon)]$ by Remark 2. By Remark 1, there is a compact set Ω_c'' with Ω_c' in the interior of it, such that for $T' \leqslant t < T$, $(w, \bar{w}, z) \in \Omega_c''$.

While $(w, \bar{w}, z, \eta) \in \Omega_c'' \times \{W(\eta) \leqslant \varepsilon^2 c_1\}$, we have $\eta = O(\varepsilon)$, and thus

$$\psi(\hat{x},\hat{\sigma}) = \psi(x,\hat{\sigma}) + O(\varepsilon) \tag{37}$$

$$\hat{\sigma} = \Delta^b(x,z,d) + \Delta^a(x,z,d)\bar{M}\begin{bmatrix} g_\varepsilon(\psi_1(x,\hat{\sigma})/M_1) \\ \vdots \\ g_\varepsilon(\psi_p(x,\hat{\sigma})/M_p) \end{bmatrix} + O(\varepsilon) \tag{38}$$

By (19), it follows that

$$\psi(x,\hat{\sigma}) = \hat{a}^{-1}(x)\left(-\hat{\sigma} - \hat{b}(x) - Kw\right)$$

From which and (38), we can show that

$$\psi(x,\hat{\sigma}) = a^{-1}(x,z,d)\left(-b(x,z,d) - Kw\right)$$

holds up to an $O(\varepsilon)$ error. Hence, we have

$$\psi(\hat{x},\hat{\sigma}) = a^{-1}(x,z,d)\left(-b(x,z,d) - Kw\right) + O(\varepsilon)$$

For $(w, \bar{w}, z) \in \Omega_c''$, i.e., in the linear region of saturation function, the closed-loop system, under feedback law $u = \psi(\hat{x},\hat{\sigma})$, can be represented as follows

$$\dot{x} = (A - BKE)x + O(\varepsilon) \tag{39}$$

$$\dot{z} = f_0(x,z) \tag{40}$$

$$\varepsilon\dot{\eta} = \Lambda\eta - \bar{B}_1\Delta_1\bar{C}\eta + O(\varepsilon) \tag{41}$$

After the interval $T_1(\varepsilon)$, the partial state η will reach the set $\{W(\eta) \leqslant \varepsilon^2 c_1\}$, even if the initial value $\eta(0)$ is outside the set. Then for $T_1(\varepsilon) \leqslant t \leqslant T$, $x(t)$ satisfies (39). If $x^*(0) = x(0)$ then we have

$$x(t) - x^*(t) = O\left(T_1(\varepsilon)\right), \quad \text{for } 0 \leqslant t \leqslant T_1(\varepsilon) \tag{42}$$

thus, $x(T_1(\varepsilon)) - x^*(T_1(\varepsilon)) = O(T_1(\varepsilon))$. Due to the continuous dependence of the solutions of differential on initial conditions and parameters, it is concluded that

$$x(t) - x^*(t) = O(\varepsilon) + O\left(T_1(\varepsilon)\right), \quad \text{for } T_1(\varepsilon) \leqslant t \leqslant T \tag{43}$$

Eqs. (42) and (43) lead to

$$x(t) - x^*(t) = O(\varepsilon) + O\left(T_1(\varepsilon)\right), \quad \text{for } 0 \leqslant t \leqslant T \tag{44}$$

Since $\lim_{\varepsilon\to 0} T_1(\varepsilon) = 0$, we have $\|x(t) - x^*(t)\| \to 0$ as $\varepsilon \to 0$. For a given set of initial conditions S_x^0 and a given $\delta > 0$, an acceptable K can guarantee that $\|w^*(t)\| = \|Ex^*(t)\| < \delta/2$, $T^* < t < T$, for some time $T^* < T$. By (44), we can choose ε small enough such that $\|x(t) - x^*(t)\| < \delta/2$, thus $\|w(t) - w^*(t)\| < \delta/2$. Then we have

$$\begin{aligned} \|w(t)\| &= \|w^*(t) + w(t) - w^*(t)\| \\ &\leqslant \|w^*(t)\| + \|w(t) - w^*(t)\| \\ &< \frac{\delta}{2} + \frac{\delta}{2} = \delta, \quad \text{for } T^* < t < T \end{aligned}$$

with which the proof is concluded.

References

[1] Jason L. Speyer, D. Kevin, Minjea Tahk, Passive homing missile guidance law based on new target maneuver models, AIAA J. Guid. Contr. Dynam. 13 (5) (1990) 803–812.

[2] Taek Lyul Song, Observability of target tracking with bearings-only measurements, IEEE Trans. Aerospace Electron. Systems 32 (4) (1996) 1268–1472.

[3] S.E. Talole, S.B. Phadke, Nonlinear target state estimation in homing guidance, in: AIAA Guidance, Navigation and Control Conference and Exhibit, Nonterey, CA, August, 2002, AIAA 2002-4772.

[4] F. Esfandiari, H.K. Khalil, Output feedback stabilization of fully linearizable systems, Internat. J. Control 56 (1992) 1007–1037.
[5] Ahmad N. Atassi, H.K. Khalil, A separation principle for the stabilization of a class of nonlinear systems, IEEE Trans. Automat. Control 44 (9) (1999) 1672–1687.
[6] Hassan K. Khalil, High-gain observers in nonlinear feedback control, in: Int. Conf. on Control, Automation and Systems, Seoul, Korea, 2008.
[7] Leonid B. Freidovich, Hassan K. Khalil, Performance recovery of feedback-linearization-based designs, IEEE Trans. Automat. Control 53 (10) (2008) 2324–2334.
[8] Taek Lyul Song, Tae Yoon Um, Practical guidance for homing missiles with bearings-only measurements, IEEE Trans. Aerospace Electron. Systems 32 (1) (1996) 434–443.
[9] K.R. Babu, K.N. Swamy, Switched biased proportional navigation for homing guidance against highly maneuvering targets, AIAA J. Guid. Contr. Dynam. 17 (3) (1994) 1357–1363.
[10] P. Zarchan, Tactical and Strategic Missile Guidance, American Institute of Aeronautics & Astronautics, 1997.
[11] Scott Bezick, Ilan Rusnak, W. Steven Gray, Guidance of a homing missile via nonlinear geometric control methods, AIAA J. Guid. Contr. Dynam. 18 (3) (1995) 441–448.
[12] V.I. Vorotnikov, Partial Stability and Control, Birkhauser, Boston, 1998.
[13] Iliya V. Miroshnik, Attractors and partial stability of nonlinear dynamical systems, Automatica (2004) 473–480.
[14] VijaySekhar Chellaboina, Wassim M. Haddad, A unification between partial stability and stability theory for time-varying systems, IEEE Control Syst. Mag. (2002) 66–75.
[15] Jang Gyu Lee, Hyung Seok Han, Young Jin Kim, Guidance performance analysis of Bank-to-Turn (BTT) missiles, in: Proc. 1999 IEEE Intern. Conf. Control Applications, Kohala Coast-Island, Hawaii, August, 1999, pp. 991–996.
[16] H.K. Khalil, Nonlinear Systems, 3rd edition, Prentice-Hall, Upper Saddle River, NJ, 2002.
[17] Jeffrey H. Ahrens, Hassan K. Khalil, High-gain observers in the presence of measurement noise: a switched-gain approach, in: Proc. 17th Congress IFAC, Seoul, Korea, 2008, pp. 7606–7611.
[18] Zhou Di, Zou Xin-Guang, Sun De-Bo, Sliding-mode guidance law for homing-missiles breaking through defense with maneuver, J. Astronaut. 27 (2) (2006) 213–216.
[19] Rafael Yanushevsky, Modern Missile Guidance, CRC Press, Taylor & Francis Group, London, 2007.
[20] George M. Siouris, Missile Guidance and Control Systems, Springer, 2003.